Macromolecules
ARTICLE

Macromolecules **2009**, *42*, 4769–4774 **4769**
DOI: 10.1021/ma802823j

Multilamellar Interface Structures in Nafion

Joseph A. Dura*

NIST-Center for Neutron Research, Gaithersburg, Maryland 20899

Vivek S. Murthi

UTC Power Corp., South Windsor, Connecticut 06074

Michael Hartman

Nuclear Engineering and Radiological Sciences, University of Michigan, Ann Arbor, Michigan 48109-2104

Sushil K. Satija

NIST-Center for Neutron Research, Gaithersburg, Maryland 20899

Charles F. Majkrzak

NIST-Center for Neutron Research, Gaithersburg, Maryland 20899

Received December 18, 2008; Revised Manuscript Received May 14, 2009

ABSTRACT: Neutron reflectometry measurements show that lamellar structures composed of thin alternating water-rich and Nafion-rich layers exist at the interface between SiO_2 and the hydrated Nafion film. Lamellae thickness and number of layers increase with humidity. Some lamellae remain in the film after dehydration. Multilayer lamellae are not observed for Nafion on Au or Pt surfaces. Instead, a thin partially hydrated single interfacial layer occurs and decreases in thickness to a few angstroms as humidity is reduced to zero. The absorption isotherm of the rest of the Nafion film is similar to that of bulk Nafion for all three surfaces investigated. The observed interfacial structures have implications for the performance, reliability, and improvements of fuel cell proton exchange membranes and membrane electrode assemblies.

Introduction

Fuel cells employing a polymer electrolyte membrane (PEM) such as Nafion show promise for a wide range of applications both in the transportation sector and for stationary power production due in part to their low operating temperatures. In hydrated Nafion, the hydrophobic fluorocarbon polymer backbone phase separates from the water, with the hydrophilic sulfonic acid side chains at the interface. The water/Nafion structures that result are of critical interest since ionic conduction occurs by proton transport along the sulfonic acid functional groups.[1] Many models are presented in the literature to describe these structures in bulk Nafion. In one model, at low hydration, water clusters are formed, and at higher levels of hydration these clusters become connected by hydrated filaments.[2,3] Parallel cylinders of water[4] and layered structural elements that form cross-linked water channels[5] in a polymer matrix have also been proposed. Other models consist of ribbon-like polymer aggregates, where these ribbons may pack into planar structures[6] or twist into helical fibrils.[7] Also, a lamellar model has been described.[8] It has also been noted that the water uptake of Nafion depends upon the pretreatment. Three forms can be prepared: by drying the Nafion above the glass transition temperature (shrunken form), by drying Nafion below it (normal form), or by boiling the Nafion in water (expanded form), which, in this order, have increasing adsorption of water when in contact with liquid.[9,10] This implies structural differences between the various pretreatment forms of Nafion.

Interfacial structures of water at the boundaries of the PEM are vital to understanding issues related to proton conductivity, gas diffusion, catalysis, and other phenomena that occur in the three-phase regions where the PEM, the catalyst/electrode, and gases (i.e., water vapor, fuel, and oxidizer) interact. Also, certain modes of device failure, e.g. delamination,[11] dissolution of the catalyst, irreversible changes to the reaction layer,[12] and membrane degradation,[13,14] can nucleate at the interface.

Interfaces between Nafion and additives also potentially improve hydration of Nafion, particularly at higher operating temperatures. Two methods have been proposed. One involves adding Pt containing fillers to generate water by combining crossover H with O within the membrane.[15,16] The other approach is to add hydrophilic fillers such as silica particles to trap water in the membrane.[17−19] The results presented herein strongly suggest the mechanisms of greater water retention using additives.

In this article we employ neutron reflectometry to determine the nanometer scale structures of water and Nafion in spin-coated Nafion films. We have determined that water-containing multilamellar structures occur in Nafion on thermal silicon dioxide, referred to as TO or the native oxide of Si referred to as SiO_2. However, multilamellar structures do not exist at the Pt/Nafion or Au/Nafion interfaces. Rather, a single thin layer with a larger water content compared to the majority of the Nafion film occurs at the interface with these metallic surfaces. The Nafion

*Corresponding author: e-mail dura@nist.gov; Ph 301-975-6251.

Published on Web 06/12/2009

films are otherwise bulklike, with a sorption isotherm similar to that of bulk Nafion.[20] However, for relative humidity above 60% the water uptake is dependent upon sample history or slow kinetics and does not always achieve the levels observed in the bulk. Recent molecular dynamic simulations similarly indicate the presence of local maxima in the water density near interfaces between Nafion and supporting solid surfaces.[21,22]

Experimental Section

Samples were prepared by spin-coating 1000 equiv wt Nafion at 3500 rpm onto Si substrates with various surface layers. The initial dispersion (from DuPont Fluoroproducts, Wilmington, DE[23]) of (20−22 wt %) perfluorosulfonic acid/TFE copolymer resin (in a solution of 1-propanol (40−48 wt %) water (30−38 wt %) ethyl alcohol (< 5 wt %) and mixed ethers and other VOC's (< 2 wt %)) was diluted 16:1 by volume in HPLC grade anhydrous ethanol before spin-coating. After deposition, samples were annealed in vacuum at either 60 or 150 °C (below or above the α-relaxation temperature,[24,25] T_α, respectively) for 1 h. Samples that were not vacuum-annealed do not adhere to the Si surface when placed in contact with liquid water. Six samples are reported on here. The sample names refer to the surface upon which the Nafion was deposited, followed by the annealing temperature and a letter if more than one similar sample was investigated. Nafion was deposited directly onto the native oxide after UV ozone cleaning and annealed at 60 °C, for samples SiO_2-60, SiO_2-60b, and SiO_2-60c. A similar sample, TO-60, was deposited on a 24 nm thick thermal oxide. The sample denoted Pt-60 consists of Nafion deposited on a nominally 6 nm Pt film. A gold surface was prepared for sample Au-60, by depositing 12 nm of Au onto a 2.5 nm Cr adhesion layer, before spin-coating the Nafion and annealing at 60 °C. The metallic films were deposited by magnetron sputtering.

The measurements were made in three separate sample environments. The humidity environment allowed control of water partial pressure by simultaneously controlling sample temperature and the dew point of either H_2O or D_2O. During data collection the sample temperature (ranging from 22.2 to 23.4 °C) was kept constant to within ±0.2 °C, measured by a Pt resistor on the sample stage. The dew point was controlled by a humidity generator, with Ar carrier gas delivered at typical flow rates of 0.5−2 SCFH. The gas mixture traveled ∼1 m through an insulated or heated hose to the sample environment. The temperature of the hose was maintained above the dew point to avoid condensation in the hose. Gases were vented through a flow meter to ensure constant flow of gas through the chamber at approximately atmospheric pressure. The relative humidity (RH) was monitored during data acquisition, although all reported values are determined from the sample temperature and dew point. The relative error of the dew point was assumed to be the fluctuations in the dew point as determined by the RH and temperature of the RH probe. The Al chamber temperature was also monitored using a type K thermocouple to ensure that it remained above the dew point of the applied vapor.

A vacuum environment was used to investigate the dehydration of the Nafion films. The chamber was similar in design to the

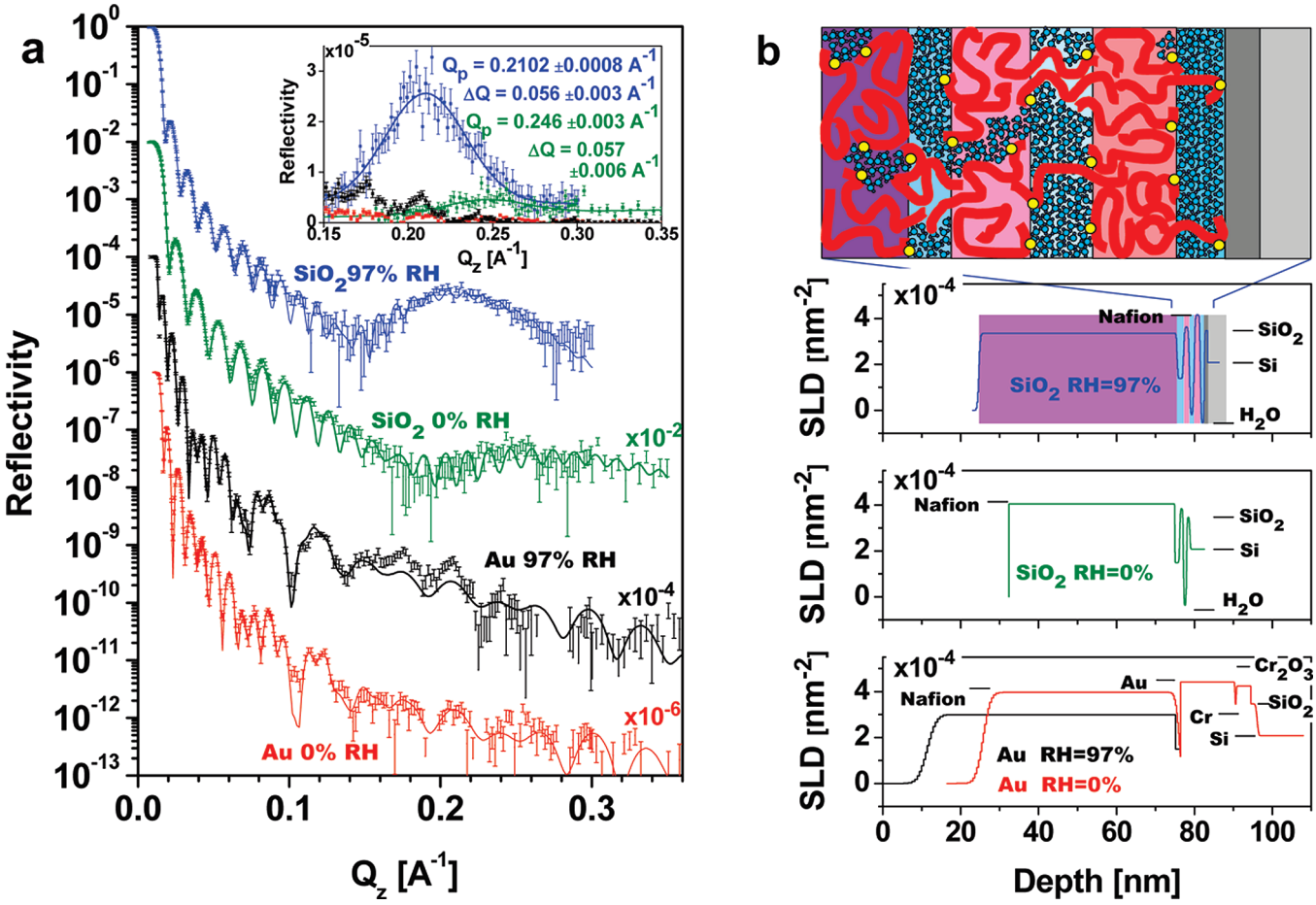

Figure 1. Specular neutron reflectivity data, fits, and models for Nafion on SiO_2 and Au. (a) Specular neutron reflectivity data and model fits showing a high-Q peak for SiO_2 at RH = 97% (blue) and a smaller high-Q peak for SiO_2 at RH = 0% (green), whereas no high-Q peak for Au with RH = 97% (black) or for Au at RH = 0 (red) is observed. (b) SLD profiles corresponding to the four fits in (a). An artist's rendition (not to scale) of the model corresponding to SiO_2-60 at RH = 97% is shown above its SLD profile with the Nafion fluorocarbon backbone in red, sulfonic acid in yellow, and water in blue.

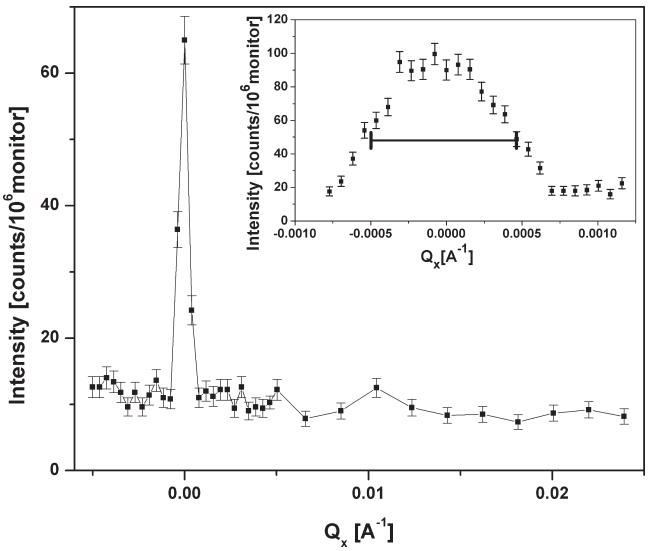

Figure 2. Transverse scan through the high-Q peak for Nafion on SiO_2 (SiO_2-60b) at RH = 58%. The inset shows the detail of the instrumental resolution limited central peak. The horizontal bar is the instrumental resolution at the slit settings used to collect the data in the inset.

humidity chamber, except that the vapor transport system was replaced with a turbo pump. The temperature was maintained to within ±0.2 °C using feedback from a Pt resistor mounted to the sample stage.

Finally, a fluids cell was used for the measurements of Nafion in contact with liquid water. The samples were sealed against a silicon block in which inlet and outlet holes were drilled, as described in the literature.[26]

Neutron reflectometry (NR)[27] data were taken using the NG1 and ANDR reflectometers[28] at the NIST Center for Neutron Research as described previously.[29] Specular NR can be fit to determine the depth profile of the neutron scattering length density (SLD), which can be interpreted as a composition depth profile when the SLD of the constituents are known. The thickness of films as thin as 1−2 nm can be measured with sub-angstrom accuracy.[30,31] Modeling employed the Parratt formalism,[32] and the "reflpak" software was used to fit the data.[33]

Results

Specular NR data are shown in Figure 1a for SiO_2-60 and Au-60 at RH = 97% (96.5% ± 1.2%) and at RH = 0 (in dry Ar) after dehydrating in Ar at 60 °C as labeled. All data were taken at a controlled temperature of 23 °C. The inset shows a portion of the data at higher Q on a linear scale. The lines in the inset are fits to a Gaussian line shape with the fit parameters displayed in the figure in the same color as the data. SiO_2-60 at RH = 97% clearly shows a peak at $Q_z = 0.2102 \pm 0.0008$ Å^{-1}, whereas no peak is seen at similar Q for any humidity for Au-60 or for Pt-60[20] (not shown). The intensity and position of this high-Q peak have a strong dependence on sample hydration, indicating that the structures that cause it involve water. For SiO_2-60 at 0% RH, the high-Q peak is considerably reduced in integrated intensity (by over a factor of 7) and has shifted to $Q_z = 0.246 \pm 0.003$ Å^{-1}, indicating a thinner structure.

The high-Q peak of SiO_2-60 at 97% RH has a full width at half-maximum (fwhm) = 0.057 ± 0.006 Å^{-1}, which is much narrower than an oscillation from a single layer could be. The position indicates that it arises from a feature roughly 3.0 nm in size while the relatively narrow width corresponds to a length of 5.6 nm, or roughly twice the feature size. This is consistent with the high-Q peak being caused by a structure composed of two repeats of the ~3 nm feature.

For transverse scans, a component of the momentum transfer lies in the plane of the sample so that in-plane structures can be probed. The transverse scan shown in Figure 2 was taken at a Q_z corresponding to this high-Q peak for a similar sample SiO_2-60b at RH = 58.0% ± 0.7%. It has a fwhm approximately equal to that expected from instrumental broadening, ΔQ_x = 0.0017 Å^{-1}, and therefore shows that the high-Q peak is predominantly specular and is likely produced from extended two-dimensional planes or lamellae. Within the instrumental sensitivity of our reflectometer we have not observed evidence for any particular in-plane structure. However, some reported in-plane structures would be inconsistent with the SLD profile of the first two lamellae determined, as follows, from fits to the specular data.

The SLD profiles determined by least-squares fits (Figure 1b) are in excellent agreement with the specular data in Figure 1a. For SiO_2-60 at RH = 97%, the layers in the model (starting with the largest depth, Z) correspond to the Si substrate, the native SiO_2 layer, and then the lamellae consisting of three water-rich layers alternating with two Nafion-rich layers. In this model the composition of the lamellae decay from nearly 100% H_2O to a final layer of ~60 vol % H_2O with increasing distance from the interface. This model confirms that the multilamellae structure, overall thickness, and average repeat distance are compatible with the peak width analysis of the high-Q peak. The thick layer above the lamellae is a layer of mixed water and Nafion with a SLD corresponding to water loading of $\lambda = 5.0 \pm 0.2$ water molecules per sulfonic acid. This thick, "majority" layer most likely consists of structures similar to those of bulk membranes.[2−8] An artist's rendition of this model (not to scale) is shown above the SLD profile in Figure 1b.

Upon dehydration, Figure 1 (green) shows that the majority of the Nafion layer on SiO_2 gets thinner and its SLD becomes approximately that of bulk Nafion. The SLD of pure Nafion indicated by the horizontal marker in Figure 1b is calculated from the bulk density of Nafion, 1.98 g/cm^3.[34] After dehydration, the lamellar structure has also been reduced in extent. Only three layers are observed, one water layer followed by one Nafion layer, and then a mixed water and Nafion layer with SLD = 1.49×10^{-4} nm^{-2}, which corresponds to ~55 vol % water.

The water content in a Nafion layer is determined from the difference in SLD between the hydrated and completely dehydrated film. Therefore, it is crucial to know the Nafion SLD in its fully dehydrated state. Two methods were used (see Supporting Information Figure S1). One method involved heating the sample to increasing temperatures until there was no more observed change in the SLD of Nafion. The other method involved comparing the SLD of dehydrated Nafion after alternately hydrating it first with H_2O and then with D_2O to identify residual water. Both methods indicate that the films are completely dehydrated at 60 °C (in dry Ar or vacuum) and that the density of the majority of the Nafion film does not assume that of the bulk for any of the films investigated but varies with sample between 1.85 and 1.93 g/cm^3. The dry Nafion SLD individually measured for each sample (when available) was used to determine the water content in the hydrated films.

In contrast to the SiO_2 surface, with Nafion spin-coated onto Au (Figure 1, black) there is no high-Q peak, and therefore multiple lamellae are not required to achieve excellent fits to the data. For RH = 97% (97.0 ± 1.2%) there is a 63.71 nm thick Nafion film with $\lambda = 7.6$ water molecules per sulfonic acid (see Figure 1b). Below this we see a single 1.25 nm mixed layer with a composition of 45% Nafion and 55% water followed by the solid sublayers, a 14.01 nm layer of Au followed by 0.33 nm of Cr, and a 3.73 nm Cr suboxide layer with SLD between that of Cr and

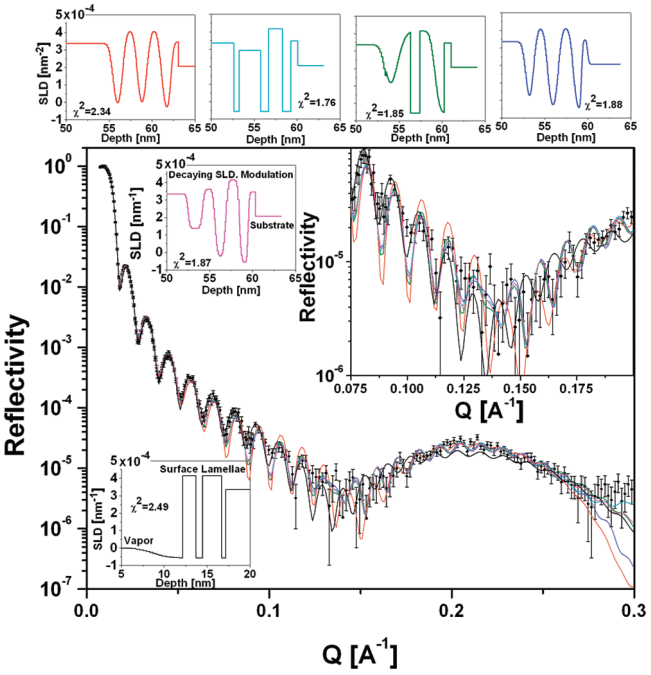

Figure 3. Several model fits (solid lines) to SiO_2-60 at RH = 97%. The corresponding SLD profiles are plotted in the smaller graphs in the same color. The large inset shows details, and the magenta SLD profile inset shows the decayed composition modulation model. The black SLD profile inset shows a symmetry-related model with the lamellae constrained to the surface.

Cr_2O_3. This Cr suboxide layer is occasionally observed when using a sputter source with a surface oxide. Below this layer is the 1.62 nm native oxide on the Si substrate. After dehydration in flowing Ar at 60 °C the Nafion achieves a SLD similar to that observed on SiO_2 (corresponding to a density of 1.89 g/cm^3), and the trapped water layer reduces to a sharp interface layer as seen in Figure 1b (red), while the sublayers remain unaltered. Measurements on Pt show similar results with only a single water-rich layer and bulklike water uptake.[20]

Because the high-Q peak contains a limited amount of information compared to the large number of parameters that can describe the five layers that make up the lamellar structure of SiO_2-60 at RH = 97%, many alternative models similar to that shown in Figure 1b (blue) can fit the data nearly as well. Figure 3 shows several such multilayer lamellae SLD profiles produced by least-squares refinement from different initial values of thickness and SLD of the layers, along with their chi squared values. The calculated reflectivities corresponding to these models are shown in Figure 3 with the same color as the models. As seen from the similarity of the fits, each of these alternative models are nearly equally possible. Therefore, while the exact composition and thickness of individual layers are beyond the ability of NR to distinguish, the features that all these fits have in common can be considered to represent the lamellar structure. Consequently, the lamellae in Nafion on SiO_2 at RH = 97% can be considered to be composed of five layers, oscillating in composition, beginning with ~100% H_2O, separated by layers with compositions closer to Nafion. This large water and Nafion content of the first two layers is not consistent with a planar arrangement of spherical clusters separated by the Nafion matrix in these initial layers. The lamellar region spans a total thickness of 6.48−6.92 nm depending upon the model.

Also, symmetry-related models can often fit NR data equally well. In the case of SiO_2-60 at RH = 97%, a model with the lamellae at the surface, as shown by the black solid line in Figure 3, fit nearly as well as fits with the lamellae at the interface.

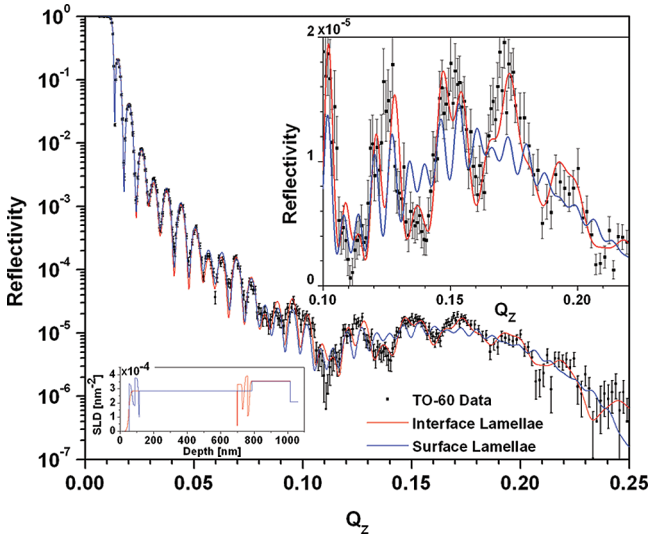

Figure 4. Specular reflectivity data for Nafion on a thermal oxide in RH = 92%. The red solid line is the best fit to the data and has lamellae at the interface. The blue solid line is a best fit to the data assuming lamellae at the surface but cannot reproduce the key oscillations as shown in detail in the inset.

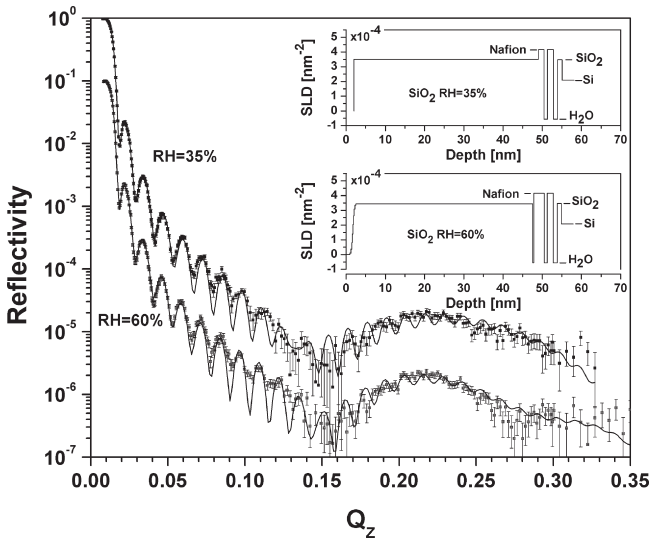

Figure 5. Specular neutron reflectivity data and model fits for Nafion on SiO_2 at intermediate humidities. The high-Q peak is seen for sample SiO_2-60 at RH = 60% (bottom) and 35% (top). The insets are the SLD profiles corresponding to model fits.

However, since the only difference between SiO_2-60 and Au-60 (with no high-Q peak) is the composition of the interface, it is likely that lamellae are induced by and are therefore located at this interface. However, it is possible to distinguish lamellae located at the surface from lamellae located at the interface by investigating a sample of Nafion deposited onto a thicker oxide film. NR oscillations from a thick oxide layer will have a greater amplitude if the oxide is next to the water-rich lamellae rather than hydrated Nafion because there is a much greater contrast between SiO_2 and water than between SiO_2 and hydrated Nafion. NR data for a sample with a 24 nm thick thermal oxide layer, TO-60, at RH = 92.3% ± 1.1%, shown in Figure 4 have large oscillations with a period of $\Delta Q = 0.026$ Å^{-1}, corresponding to the oxide thickness. Excellent fits to the data (red solid line) are achieved for models with lamellae at the interface. However, in best fits when the lamellae are restricted to the surface, the ΔQ =

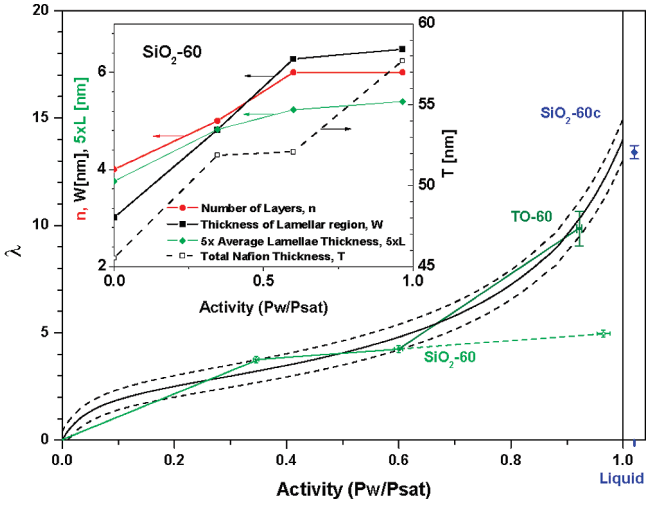

Figure 6. Sorption isotherm for the majority portion of the Nafion (data points) compared to the solid line taken from the literature for bulk Nafion. The dashed lines roughly indicate the uncertainty in literature values and are placed at $\lambda(1 \pm 0.4) \pm 0.4$ Also shown in the inset are additional details as a function of RH as indicated.

0.026 $Å^{-1}$ oscillations cannot be reproduced (blue solid line). This strongly suggests that the lamellae are located at the interface between the Nafion and the substrate layers.[35]

The high-Q peak was also observed in multiple samples with SiO_2 surfaces over a wide range of relative humidities. Fits to data taken for sample SiO_2-60 at 35% (34.6% ± 0.5%) and 60% (60.0% ± 0.8%) relative humidity (Figure 5) show that the number of water layers continuously increases with increasing RH as seen in SLD profiles displayed as insets to Figure 5. At RH = 35%, four lamellae are formed, with a total thickness of 4.82 nm. At RH = 60% the models indicate that five lamellae occur over a distance of 6.28 nm total.

In Figure 6 the sorption isotherm for the (nonlamellar) majority of Nafion on SiO_2 is compared to the values of a curve fit to bulk films, obtained from the literature.[36] Unless otherwise noted, the error bars are calculated assuming that the uncertainty of all SLD values equals the standard deviation of the majority Nafion SLD values for the models seen in Figure 3. The water uptake for SiO_2-60 (determined using the SLD for dry Nafion measured for this sample) follows bulk values closely through RH = 60%. At 97% the water uptake for SiO_2-60 falls short of the bulk isotherm. However, at a similar humidity, TO-60 shows bulklike water uptake. Since a measurement of dehydrated TO-60 is unavailable, the average measured dry Nafion SLD was used, and the standard deviation of this average was used in calculating the error bars for TO-60. These error bars represent the uncertainty for all λ taking into account observed variations in the dry Nafion density.

The reduced uptake for SiO_2-60 at RH = 97% may be due to kinetics, in agreement with the literature.[10] Sample equilibrium during data acquisition was ensured by using only sequential data files that did not vary within statistical uncertainty. In some samples several hours were required to reach equilibrium. For example, another sample of Nafion on SiO_2 (SiO_2-150, not shown) which was annealed at 150 °C and then placed in D_2O liquid had appeared stable at a thickness of ~86 nm but then increased to ~96 nm when left in D_2O for 13 days between measurements. SiO_2-60 was studied for 8 h while TO-60, which had greater adsorption of water, remained in 97% RH for 24 h before the data were taken over a similar 8 h period. In both cases water uptake was stable during the entire measurement period. This indicates a possible delayed onset for water uptake in thin films on SiO_2 at higher activity. It appears, however, that at longer times the water uptake is similar to bulk Nafion membranes.

Data for SiO_2-60c in liquid water is placed beyond RH = 100% in Figure 6 for clarity. In liquid water, this sample absorbed $\lambda = 13.4 \pm 0.3$ water molecules per sulfonic acid. This corresponds to what is observed in bulk membranes for a similar pretreatment. While bulk Nafion samples with equivalent weight of 1100 prepared in boiling water (the expanded form) reach λ in the range of 22−23,[37] samples heated at 80 °C in a dry environment (the normal form) reach $\lambda = 13$[9] and samples annealed at 105 °C (the shrunken form) reach $\lambda = 11$.[9] Since the water content increases with lower annealing temperature, the value measured for SiO_2-60c is similar to the values measured in bulk membranes.

Discussion

In this article we have shown that single water-rich lamellae occur at the interface between Nafion and the metals Au and Pt and also that a multilamellar structure occurs at the interface between SiO_2 and Nafion. This could be an interface induced ordering of the ribbon-like aggregates[6] or lamellae[5,8] observed in SAXS and SANS with the first Nafion-rich layer consisting of closely packed ribbons or lamellae oriented with their faces parallel to the substrate and with successive layers increasingly disordered. The observed structures are also consistent with the mean field theory calculations of damped composition oscillations that occur near the microphase-separation transition (MST) in block copolymers.[38] For example, in PS−PMMA copolymers the PMMA block is attracted to the Si surface, and the composition oscillates between PS and PMMA, with a decaying amplitude.[39,40] The similarity is not surprising since Nafion is a copolymer of Teflon and sulfonic acid, with the latter being decorated by water when hydrated. Dehydrating the film changes the volume ratio of the two copolymer components, which changes the period of composition oscillation L and extrapolation length (essentially W) as seen in the inset of Figure 6. Multilamellar structures are not present in Nafion on Au or Pt surfaces, but instead a single layer exists at the interface, with a much lower water content than the interfacial layer on SiO_2. This indicates that Au and Pt surfaces have a lower affinity to the sulfonic acid/water phase than the more hydrophilic SiO_2 surface. At RH = 97% the water content of this single layer on Au is similar to the outermost layer lamellae on SiO_2 (as seen in the decaying composition modulation model in Figure 1a). This would indicate that as the water content falls to roughly 50−60% the chemical potential is too low to induce additional composition oscillations.

Although the majority of the Nafion film is fully dehydrated by heating to 60 °C, a residual interfacial structure remains (up to temperatures as high as 150 °C as seen in the Supporting Information), which likely consists of three layers on SiO_2 or one extremely thin layer on metals. One possibility is that these residual structures contain water that is more tightly bound than in bulk. Another explanation is that water is trapped at the interface by a dehydrated outer Nafion film. If this were the case, it would indicate that the water lamellae are not well connected to the percolation network of the water clusters or cylinders in the majority of the Nafion film, i.e., a skin of the fluorocarbon Teflon-like backbone of Nafion forms above the lamellae which is continuous and relatively impervious. A third possible explanation is residual low-density Nafion layers, e.g., uncollapsed voids, are left in the film after the water is removed, perhaps stabilized by interactions with the rigid substrate. However, it should be noted that that these structures remain on SiO_2 when heated to 150 °C, i.e., above T_α.

While spin-coated Nafion is an idealized system selected to enable NR measurements, the structures observed herein may be

indicative of nanoscaled structures occurring at the interface between Nafion and other materials in bulk samples, e.g., catalyst electrode particles. Similarly, the multiple layers of water and Nafion observed here may also manifest as multiple shells above the additive/PEM interfaces, which may become interconnected at higher particle densities and explain the enhanced properties found with hydrophilic fillers. Finally, even if these structures occur only in thin films due to effects of finite size or sample preparation techniques, these results are nonetheless beneficial for thin films technologies, such as sub-micrometer length scale thin film fuel cells used in on-chip power for stand-alone wafer scaled devices.

Conclusion

Specular and off-specular neutron reflectometry measurements show that multilamellar structures exist in Nafion spin-coated onto SiO_2 surfaces. Models obtained from fitting the specular neutron reflectometry data indicate that the lamellae are composed of thin alternating water-rich and Nafion-rich layers at the interface between SiO_2 and the hydrated Nafion film. Both the lamellae thickness and number of layers increase with humidity. Some lamellae remained in the film after dehydration. Multilayer lamellae are not observed for Nafion on Au or Pt surfaces. Instead, a thin, partially hydrated single interfacial layer occurs and decreases in thickness to a few angstroms as humidity is reduced to zero. The absorption isotherm of the rest of the Nafion film is similar to that of bulk Nafion for all three surfaces investigated.

Acknowledgment. The authors acknowledge the assistance of Paul Kienzle with some of the reflectivity modeling and both Jon Owejan and Timothy Fuller for useful discussions and for supplying the Nafion dispersion. Some samples were made in part at the NIST Center for Nanoscale Science and Technology.

Supporting Information Available: Two methods used to demonstrate that Nafion films are fully dehydrated by heating to 60 °C in vacuum or flowing Ar; data also indicate that Nafion film density at 23 °C decreases with increasing temperature of vacuum heating. This material is available free of charge via the Internet at http://pubs.acs.org.

References and Notes

(1) Weber, A. Z.; Newman, J. *J. Electrochem. Soc.* **2003**, *150*, A1008–A1015.
(2) Gierke, T. D.; Munn, G. E.; Wilson, F. C. *J. Polym. Sci., Polym. Phys. Ed.* **1981**, *19*, 1687–1704.
(3) Gebel, G. *Polymer* **2000**, *41*, 5829–5838.
(4) Schmidt-Rohr, K.; Chen, Q. *Nat. Mater.* **2008**, *7*, 75–83.
(5) Haubold, H.-G.; Vad, Th.; Jungbluth, H.; Hiller, P. *Electrochim. Acta* **2001**, *46*, 1559–1563.
(6) Rubatat, L.; Rollet, A. L.; Gebel, G.; Diat, O. *Macromolecules* **2002**, *35*, 4040–4055.
(7) Chomakova-Haefke, M.; Nyffenegger, R.; Schmidt, E. *Appl. Phys. A: Solids Surf.* **1994**, *59*, 151–153.
(8) Litt, M. H. *Polym. Prepr.* **1997**, *38*, 80–81.
(9) Hinatsu, J. T.; Mizuhata, M.; Takenaka, H. *J. Electrochem. Soc.* **1994**, *141*, 1493–1498.
(10) Onishi, L. M.; Prausnitz, J. M.; Newman, J. *J. Phys. Chem. B* **2007**, *111*, 10166–10173.
(11) Kim, S.; Mench, M. M. *J. Power Sources* **2007**, *174*, 206–220.
(12) Xie, J.; Wood, D. L.III; Wayne, D. M.; Zawodzinski, T. A.; Atanassov, P.; Borup, R. L. *J. Electrochem. Soc.* **2005**, *152*, A104–A113.
(13) Laconti, A. B.; Hamdan, M.; McDonald, R. C. In *Handbook of Fuel Cells - Fundamentals, Technology and Applications*; Vielstich, W., Lamm, A., Gasteiger, H. A., Eds.; John Wiley & Sons: New York, 2003; Vol. 3, p 647.
(14) Sompalli, B.; Litteer, B. A.; Gu, W.; Gasteiger, H. A. *J. Electrochem. Soc.* **2007**, *154*, B1349−B1357 and references therein.
(15) Xing, D.-M.; Yi, B.-L.; Fu, Y.-Z.; Liu, F.-Q.; Zhang, H.-M. *Electrochem. Solid State Lett.* **2004**, *7*, A315–A317.
(16) Zhu, X.; Zhang, H.; Zhang, Y.; Liang, Y.; Wang, X.; Yi, B. *J. Phys. Chem. B* **2006**, *110*, 14240–14248.
(17) Adjemian, K. T.; Lee, S. J.; Srinivasan, S.; Benziger, J.; Bocarsly, A. B. *J. Electrochem. Soc.* **2002**, *149*, A256–A261.
(18) Arico, A. S.; Baglio, V.; Di Blasi, A.; Creti, P.; Antonucci, P. L.; Antonucci, V. *Solid State Ionics* **2003**, *161*, 251–265.
(19) Nicotera, I.; Zhang, T.; Bocarsly, A.; Greenbaum, S. *J. Electrochem. Soc.* **2007**, *154*, B466B473.
(20) Murthi, V. S.; Dura, J. A.; Satija, S. K.; Majkrzak, C. F. *ECS Trans.* **2008**, *16*, 1471–1485.
(21) Selvan, M. E.; Liu, J.; Keffer, D. J.; Cui, S.; Edwards, B. J.; Steele, W. V. *J. Phys. Chem. C* **2008**, *112*, 1975–1984.
(22) Liu, J.; Selvan, M. E.; Cui, S.; Edwards, B. J.; Keffer, D. J.; Steele, W. V. *J. Phys. Chem. C* **2008**, *112*, 1985–1993.
(23) Certain commercial equipment, instruments, or materials (or suppliers, or software, etc.) are identified in this paper to foster understanding. Such identification does not imply recommendation or endorsement by the National Institute of Standards and Technology, nor does it imply that the materials or equipment identified are necessarily the best available for the purpose.
(24) Osborn, S. J.; Hassan, M. K.; Divoux, G. M.; Rhoades, D. W.; Mauritz, K. A.; Moore, R. B. *Macromolecules* **2007**, *40*, 3886–3890.
(25) Page, K. A.; Cable, K. M.; Moore, R. B. *Macromolecules* **2005**, *38*, 6472–6484.
(26) Krueger, S.; Meuse, C. W.; Majkrzak, C. F.; Dura, J. A.; Berk, N. F.; Tarek, M.; Plant, A. L. *Langmuir* **2001**, *17*, 511–521.
(27) Majkrzak, C. F. *Acta Physiol. Pol.* **1999**, *A96*, 81–99.
(28) Dura, J. A.; Pierce, D. J.; Majkrzak, C. F.; et al. *Rev. Sci. Instrum.* **2006**, *77*, 074301−1–074301−11.
(29) Jach, T.; Dura, J. A.; Nguyen, N. V.; Swider, J.; Cappello, G.; Richter, C. *Surf. Interface Anal.* **2004**, *36*, 23–29.
(30) Dura, J. A.; Richter, C. A.; Majkrzak, C. F.; Nguyen, N. V. *Appl. Phys. Lett.* **1998**, *73*, 2131–2133.
(31) Seah, M. P.; Spencer, S. J.; Bensebaa, F.; et al. *Surf. Interface Anal.* **2004**, *36*, 1269–1303.
(32) Parratt, L. G. *Phys. Rev.* **1954**, *95*, 359–369.
(33) Kienzle, P. A.; O'Donovan, K. V.; Ankner, J. F.; Berk, N. F.; Majkrzak, C. F. http://www.ncnr.nist.gov/reflpak, **2000−2006**.
(34) DuPont Nafion PFSA membranes N-115, N-117, and N-1110 (technical document Copyright 2008 DuPont or its affiliates).
(35) An alternative description has been also modeled though not fit to the data. In this model the sample is described as consisting of many individual subsamples in which a single five-layer set of lamellae are placed at different depths ZL from the SiO_2 within the Nafion film. Since, in this model, these subsamples are larger than the neutron coherence length in the plane of the sample, the scattering from each subsample will add incoherently; i.e., the intensities will be added. (If the individual layers were smaller than the coherence length of the neutron, only the average in-plane composition would contribute to the scattering.) Models with narrow distributions of ZL centered away from either interface show a beating pattern of the oscillations, similar to the single sample models discussed in the text, which is also not consistent with the data. Broader distributions do not have such a beating pattern, but the intensity of the oscillations of the summed intensity fall under an envelope function which includes a broad peak at roughly half the Q value of the high-Q peak, which is not seen in the data, indicating that this model is not as good a fit to the data as one with a single set of lamellae located at the interface or surface of the Nafion film.
(36) Choi, P.; Jalani, N. H.; Datta, R. *J. Electrochem. Soc.* **2005**, *152*, E84–E89.
(37) Choi, P.; Datta, R. *J. Electrochem. Soc.* **2003**, *150*, E601–E607.
(38) Fredrickson, G. H. *Macromolecules* **1987**, *20*, 2535–2542.
(39) Anastasiadis, S. H.; Russell, T. P.; Satija, S. K.; Majkrzak, C. F. *Phys. Rev. Lett.* **1989**, *62*, 1852–1855.
(40) Menelle, A.; Russell, T. P.; Anastasiadis, S. H.; Satija, S. K.; Majkrzak, C. F. *Phys. Rev. Lett.* **1992**, *68*, 67–70.